Assessment of Mechanical Properties of Wood-Leather Panels and the Differences in the Panel Structure by Means of X-Ray Computed Tomography

Stefanie Wieland,[a,*] Tilman Grünewald,[a,c] Sven Ostrowski,[a] Bernhard Plank,[b] Gernot Standfest,[a] Brigitte Mies,[a] and Alexander Petutschnigg [a]

Wet-white and wet-blue leather shavings were investigated as promising new raw materials as they seem to offer a high availability and cost competitiveness compared to wood, and they also show some interesting new properties. In order to determine a new field of application for the leather shavings and to understand the fiber particle interaction, boards with a density of 700 kg/m³ and a resin load of 12% were produced with varying contents of wood fibers, wet-blue and wet-white leather particles. These panel composites were characterized with regard to their internal bond, modulus of elasticity, and modulus of rupture. Furthermore, the micro-structure of selected panels was investigated by X-Ray computed tomography (CT). Different phases within the CT data were segmented using thresholding algorithms, and the pore size distribution of the panels was analyzed. A substantial difference was found between the panels produced due to the incorporation of leather particles. The internal bond strength increased with rising leather particle content, whereas other mechanical properties dropped. The CT analysis showed a huge difference in the pore size distribution and the number of pores for the different materials. This indicates that the differences visible in mechanical testing were induced by the different geometry of the constituents.

Keywords: Wet-blue leather; Wet-white leather; MDF; Mechanical properties; X-Ray computed tomography; Pore size distribution

Contact information: a: Department of Forest Products Technology & Construction, University of Applied Sciences Salzburg, 136a Marktstrasse, A-5431, Kuchl, Austria; b: University of Applied Sciences Upper Austria, 23 Stelzhamerstrasse, A-4600 Wels, Austria; c: Department of Materials Science and Process Engineering, Institute for Physics and Material Sciences, BOKU – University of Natural Resources and Life Sciences, Peter Jordan Straße 82, 1190 Vienna, Austria;
** Corresponding author: stefanie.wieland@fh-salzburg.ac.at*

INTRODUCTION

The increasing scarcity in the raw material supply for wood-based panels has triggered recent developments that seek to diversify the supply sources of lignocellulosic material. Materials such as rice husks (Leiva *et al.* 2007), straw (Han *et al.* 2001), bagasse, and bamboo (Lee *et al.* 2006) have the potential to substitute for a certain amount of raw material, but their share is still small compared to the overall production of 65 mio. m³ of wood-based panels (European Panel Federation 2008) and 20 mio. m³ of medium density fiberboard (Botting 2011) in Europe. This current balance in the wood supply will change dramatically within the coming years. Mantau (2010) predicts a worldwide undersupply of roughly 100 mio. m³ of woody biomass in the year 2020.

In this paper, we investigate the mechanical properties of panels made from wood fibers and leather particles. Leather shavings are a by-product of the leather preparation process; the shavings are generated when a tanned hide is trimmed to its final thickness. These shavings offer special properties as, during the leather preparation/tanning, the collagen fibers in the sarcolemma are cross-linked and therefore stabilized against

mechanical wear and biological degradation (Kanagaraj *et al.* 2006). In 2007, 0.2 megatonnes of shavings were produced in Europe (LMC International 2007) with a continuing future trend. Currently this shaving material can only be disposed of in landfills, as it shows poor combustion properties. This situation and the interesting properties and characteristics of the new panels obtained during the past two years of research are the reasons for the presented paper. In the last few years, some attempts have been reported on the use of wet-blue leather either as a filler in a polyvinyl butyl matrix (Ramaraj 2006; Ambrósio *et al.* 2011) or low-grade applications, such as protein-based glues or lubricants (Sundar *et al.* 2011; Kanagaraj *et al.* 2006). Grünewald *et al.* (2012) investigated the distribution of leather and wood panels of low density by Raman spectroscopy. However, there is no current literature on the mechanical properties of fiberboards made of wood and leather, other than the European Patent issued to Lackinger (2009). Additionally, Wieland *et al.* (2012) presented specific properties of wood-leather panels regarding fire retardance, and Ostrowski (2012) reported on the use of leather shavings as an insulative material and on the water-sorption properties of the material.

All of the above-mentioned materials influence the mechanical properties of the composite panel in one way or another. Some attempts have been taken to describe the interaction of different components in a composite material. One approach of multi-scale mechanical modeling that shows good results for concrete, wood, or bone is described by Mang *et al.* (2009). A key factor for all these models is the interaction between the different elements within the material.

In the presented work on wood leather panels, considerations were not just limited to one material such as wood, but also included the combination of wood and leather. Therefore the interaction of these materials and also the distribution within the panel is important. In order to investigate the structure of materials, X-ray computed tomography (CT) is an excellent method to gain further information on parameters such as the distribution of pores or material. The minimum resolution is somewhere in the region of 1 μm, depending on the sample size. Recent research has supplied insights into the micro-structure of wood, particle board, oriented strand board (OSB) (Standfest *et al.* 2009), and medium density fiberboard (MDF) (Standfest *et al.* 2010). The most challenging task during the analysis of this data is the segmentation of the images according to the different constituents. This is mainly done by thresholding algorithms, as presented by Otsu (1979).

The aim of this paper is to investigate the influence of wet-blue and wet-white leather particles on selected mechanical panel properties when produced in combination with wood fibers. In order to understand the composition of the bulk, CT scans were used to investigate the void distribution and to see how they are affected by the respective constituents. In order to understand the difference in the mechanical behavior, an assessment on the different fracture modes was conducted.

EXPERIMENTAL

Materials

The leather material for the presented tests was specified and provided by Gerald Lackinger Consulting (Salzburg, Austria). They were derived from cattle hide and were produced during the shaving to thickness phase in the leather preparation. The wet-blue material (WB) comes from hides treated with chromium tanning, whereas the wet-white (WW) material comes from hides treated with chromium-free tanning. The material was dried to a final moisture content < 10% in a drying kiln, and the material was sieved to a particle size below 4 mm (Fig.1), prior to use.

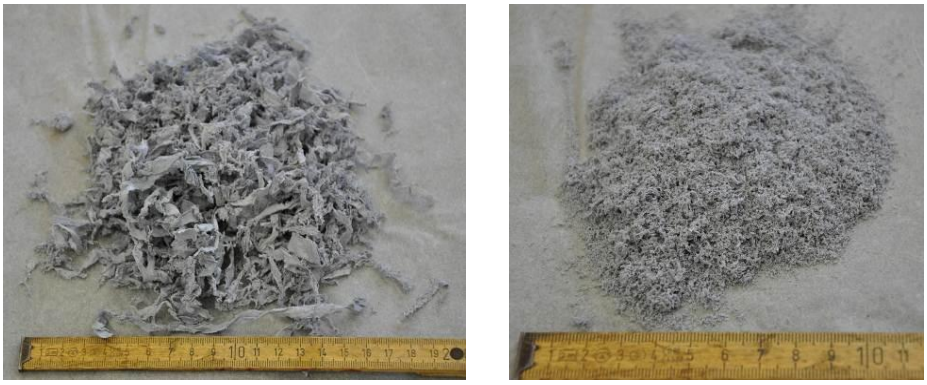

Fig. 1. Wet-blue leather shavings before (left) and after sieving (right)

As the used leather material is exclusively generated during the production of upholstery leather, the generated material is very uniform in its consistency and appearance. The WW material has a shrinkage temperature of 72°C and the WB material of 100°C on the basis of DIN-EN ISO 3380:2003 and the chromium content. For WW no chromium should be contained in the ash, according to DIN-EN ISO 5398-2:2009, whereas the WB ash can contain between 5 and 6% of chromium. The target dry weight of the finished leather was 800 to 1000 g/m². No further preservatives such as formaldehyde or pesticides were tolerated within the material.

The wood fibers were provided by MDF Hallein, (Hallein, Austria). The provided fibers were generated with a defibrator power consumption of 135 kWh/t (absolute dry/abs. dry) and were dried to a moisture range of 10.0 to 10.5%. They were exclusively derived from spruce wood (*Picea abies*) and exhibited an average fiber length of 5178 µm (555 sd) and a width of 34 µm (7 sd). All samples were prepared using an urea-formaldehyde (UF) glue Kaurit K-350 by BASF, (Ludwigshafen, Germany) with a solid content of 66%. Prior to use, 1% ammonium sulfate was added as a hardener to the K-350 resin. The final formulation showed a pH value of 6.5 and a viscosity of 280 mPaS (20 rpm/rotational viscometer)

Board Manufacture

To investigate the influence of the two different leather particle types on the properties of fiber boards, samples with varying leather content from 0% (no leather content, 100% wood fibers comparable to a standard MDF board) to 100% (100% leather content) with 25% increment steps were prepared. The resin load was 12% (abs. dry/ abs. dry) for all panels. As the resin load and production parameters were oriented on common references (Dunky and Niemz 2002), the 0% samples could be regarded as references to conventional MDF as defined by OENorm EN 622-5:2010, "MDF Generals Purpose – Dry".

Two boards with 340 x 250 x 12 mm were prepared for each combination. The boards were produced using a Hoefer HLOP 280 automated hot-press with a pressing temperature of 180°C, a pressing factor of 0.5 min/mm, and with closing to final thickness (no specific pressure). The resin was sprayed with a Schlick two-substance nozzle with a pressure of 2.5 bars; the resin was fed gravimetrically with a cup. As fiber-resin agglomerates, being an obstacle for the mechanical properties, the resinated fiber material was soaked with a conventional vacuum cleaner Bosch GAS 50-M. During this procedure the material for one panel was soaked with a constant feed to the vacuum cleaner. This procedure separates the agglomerates and ensures even glue spread and resembles the conditions in the blow-line of the MDF production. Afterwards the fiber material showed a fluffy appearance and could be used directly for the fibre mat

preparation. The treatment was carried out for all specimens to create equal production conditions. The moisture content measurements of the material prior and after this treatment showed that no significant loss of resin occurred.

Specimen Preparation

Sample sets for internal bond strength (IB) testing, the determination of the modulus of rupture (MOR), and modulus of elasticity (MOE) were prepared from the laboratory produced boards. In order to eliminate edge effects, all panels were trimmed to 220x300 mm and subsequently four strips of 300x50 mm were cut out of one panel for each combination. One of the middle strips of each panel was used for the determination of the IB strength. Prior to testing, all specimens were stored at a climate of 20°C and 65 % relative humidity (r.h.) until the equilibrium moisture content was reached.

Mechanical Testing

The determination of the mechanical properties of the boards was performed on a ZwickRoell Z 250 universal testing machine.

Internal Bond

The IB strength was determined according to OENORM EN 319:2005. A total of 10 samples was tested for each combination. Therefore five samples of 50x50 mm were cut from each strip (300x50 mm) of the two similar panels of each combination. The specimens were tested until failure with a continuous crosshead-speed of 0.5 mm/min.

Modulus of rupture

The MOR was evaluated according to OENORM EN 310:2005. A total of six samples of 300x50 mm were tested for each of the two similar panels of each combination. The specimens were tested with a continuous crosshead-speed of 10 mm/min.

Modulus of elasticity

The MOE was evaluated according to OENORM EN 310:2005. A total of six samples of 300x50 mm were tested for each of the two similar panels of each combination. The specimens were tested with a continuous crosshead-speed of 10 mm/min. The MOE was obtained from the linear values between 30 to 40% of the maximal load.

Statistical data evaluation

The obtained data were statistically treated. In order to check the influence of the density compared to the leather content on the mechanical properties an Analysis of Variance (ANOVA) with density as covariate was used to determine the explanatory effect of each parameter on the model (Backhaus *et al.* 2005).

To determine statistical differences as a function of the leather content, a one-way Welch-ANOVA was carried out to compare the differences between the groups of leather contents for WW and WB (Backhaus *et al.* 2005). The analyses were carried out using PASW Statistics ® 18 software package. The general level of significance was 0.05.

X-Ray Computed Tomography

For the investigations on the bulk structure of the material, two samples with a wet-blue content of 25% and 75% and a volume of about 3 x 3 x 12 mm^3 were scanned by X-ray computed tomography (CT). The X-ray tomograms were scanned using a Nanotom 180 NF CT device, constructed by GE phoenix/X-ray (Wunstorf, Germany) with a 180 kV nano focus tube and a 2300 x 2300 pixel Hamamatsu detector

(Hamamatsu City, Japan). The target used was made of molybdenum. The used resolution (volumetric pixel/voxel size) was 7.5 μm, the voltage at the nano focus tube was 50 kV, the measurement current was 300 μA, and the integration time at the detector was 750 ms. Altogether 1,600 projections were recorded, which led to a total measurement time of about 140 min. For image reconstruction, a filtered back-projection algorithm was applied by using the Nanotom reconstruction software datos X. No further artifact correction, such as beam-hardening correction of the CT data, or any kind of filter methods to reduce the noise, was carried out. In contrast to medical CT scanners for industrial CT, no calibrated gray values (absorption coefficients) for the raw materials (wood and leather) were used. The main target of the image segmentation of the different materials, were readily distinguishable without calibrated values.

Thresholding and segmentation

As the panels consist of wood fibers and leather particles, the whole system can be regarded as a three-phase system with the following components: wood, leather, and void. It is optically apparent that leather and wood have different absorptions, which are represented by different gray levels of the pixels. With respect to Standfest *et al.* (2009) and Otsu (1979), a thresholding algorithm was applied, aiming to maximize the variance between the three classes, or minimize the variance within a class. This is done by interpreting the three phases as an estimation of two boundary limits *t1* and *t2*. For the present case, the distribution of each phase is considered as normal. The limits *t1* and *t2* are preferred where the heterogeneity in each phase is low and the differences between the phases are high. As these assumptions show strong similarities to the assumptions necessary for the Analysis of Variance (ANOVA), this tool was used to evaluate the difference between the three classes.

In further steps, this algorithm was iterated until a maximum in class difference was found. To eliminate biasing by artifact and surface effects, an image-stack with dimensions of 263 x 298 x 1523 voxels, representing a volume of 1.972 x 2.235 x 11.422 mm³ was selected for the further 3D image analysis.

3D-image analysis

For further considerations regarding the fracture mode of the different materials, the number and sizes of the pores in the material can give valuable information. This is because the different ratios of materials lead to altered packing of the material. For instance, a volume composed of small particles will have more but small pores, whereas the same volume composed of larger particles will have fewer but larger pores. This model can be transferred to the two constituent system of wood fiber and leather particles.

In order to analyze the 3D-pore-size distribution of the panels, a method presented by Standfest *et al.* (2010) was used. The method is based on incorporating a sphere-shaped structuring element within the pore space of the greyscale image. After each operation the pores filled by the structuring element are deleted and the structuring element is enlarged by two voxels in each spatial direction (shown in Fig. 2). This method is called 'opening' size distribution. With basic morphological operations (erosion and dilation), the pore sizes and pore distributions can be determined. This method was originally established by Matheron (1975) and Serra (1982). For further data processing, binary images were calculated according to the segmentation algorithm described in the section of *Thresholding and segmentation* by using MATLAB 2009. The 3D pore size distribution was also carried out with MATLAB 2009 and a spherical structuring element.

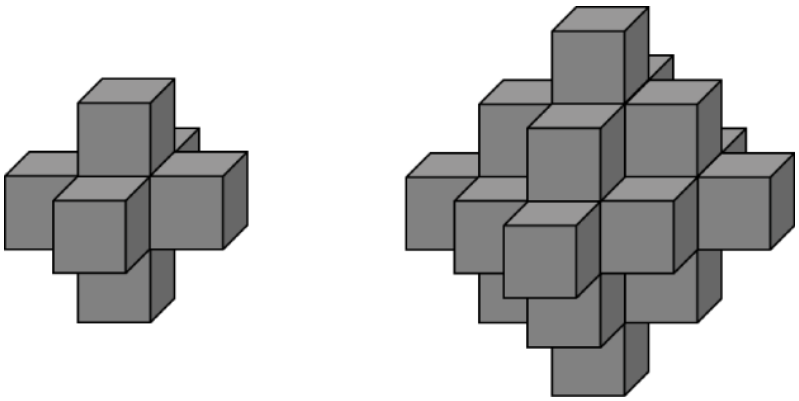

Fig. 2. Growth of the structuring element

RESULTS

Mechanical Properties

Table 1 gives an overview of the obtained values of the mechanical properties of the panels and their respective standard deviation (sd) and number of specimens {n}.

Table 1. Mechanical Properties of the WB and WW Fiber Boards

Wood [%]	Leather [%]	IB [N/mm²] (sd) {n}	MOE [N/mm²] (sd) {n}	MOR [N/mm²] (sd) {n}	Density [kg/m³] (sd) {n}
100	0	0.47 (0.05) {10}	3773 (337) {6}	41.6 (8.8) {6}	743 (24) {16}
75	25 WB	0.52 (0.16) {10}	2686 (569) {6}	27.7 (8.3) {6}	792 (38) {16}
50	50 WB	0.37 (0.22) {10}	1640 (449) {6}	16.0 (6.7) {6}	807 (49) {16}
25	75 WB	0.83 (0.14) {10}	1508 (180) {6}	19.4 (1.6) {6}	772 (51) {16}
0	100 WB	0.89 (0.06) {10}	893 (191) {6}	13.6 (2.2) {6}	811 (24) {16}
75	25 WW	0.29 (0.08) {10}	2312 (478) {6}	20.0 (6.1) {6}	773 (64) {16}
50	50 WW	0.91 (0.18) {10}	1976 (365) {6}	20.5 (3.2) {6}	765 (29) {16}
25	75 WW	0.99 (0.31) {10}	1297 (334) {6}	13.5 (3.1) {6}	734 (56) {16}
0	100WW	0.67 (0.15) {10}	458 (137) {6}	4.1 (1.1) {6}	723 (38) {16}

Given in Tables 2 through 7 are the p-values for the statistical comparison of the mechanical data by a Welch-ANOVA. Table 8 shows the eta^2-values for the analysis of covariance for leather content and density.

Table 2. p-Values of Welch-ANOVA for the IB of WB panels

	0	25	50	75	100
0	-	0.336	0.224	0.000	0.000
25		-	0.098	0.000	0.000
50			-	0.000	0.000
75				-	0.271

Table 3. p-Values of Welch-ANOVA for the IB of WW panels

	0	25	50	75	100
0	-	0.000	0.000	0.000	0.002
25		-	0.000	0.000	0.000
50			-	0.481	0.005
75				-	0.011

Table 4. p-Values of Welch-ANOVA for the MOR of WB panels

	0	25	50	75	100
0	-	0.019	0.000	0.001	0.000
25		-	0.023	0.057	0.007
50			-	0.279	0.421
75				-	0.001

Table 5. p-Values of Welch-ANOVA for the MOR of WW panels

	0	25	50	75	100
0	-	0.001	0.001	0.000	0.000
25		-	0.876	0.049	0.001
50			-	0.003	0.000
75				-	0.000

Table 6. p-Values of Welch-ANOVA for the MOE of WB panels

	0	25	50	75	100
0	-	0.004	0.000	0.229	0.000
25		-	0.428	0.006	0.000
50			-	0.528	0.008
75				-	0.000

Table 7. p-Values of Welch-ANOVA for the MOE of WW panels

	0	25	50	75	100
0	-	0.000	0.000	0.000	0.000
25		-	0.203	0.002	0.000
50			-	0.007	0.000
75				-	0.001

Table 8. Partial eta²-values for Analysis of Covariance

	Density	Leather content
IB WB	0.265	0.757
IB WW	0.404	0.814
MOE WB	0.387	0.937
MOE WW	0.644	0.952
MOR WB	0.142	0.792
MOR WW	0.264	0.852

Figures 3 to 5 visualize IB, MOE, and MOR with regard to the leather content for WW and WB fiberboards.

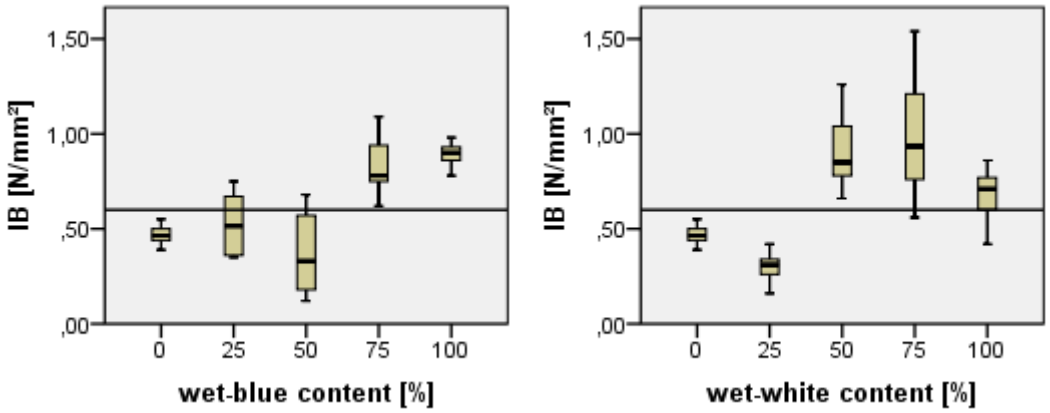

Fig. 3. Internal Bond of wet-blue (left) and wet-white fiberboard

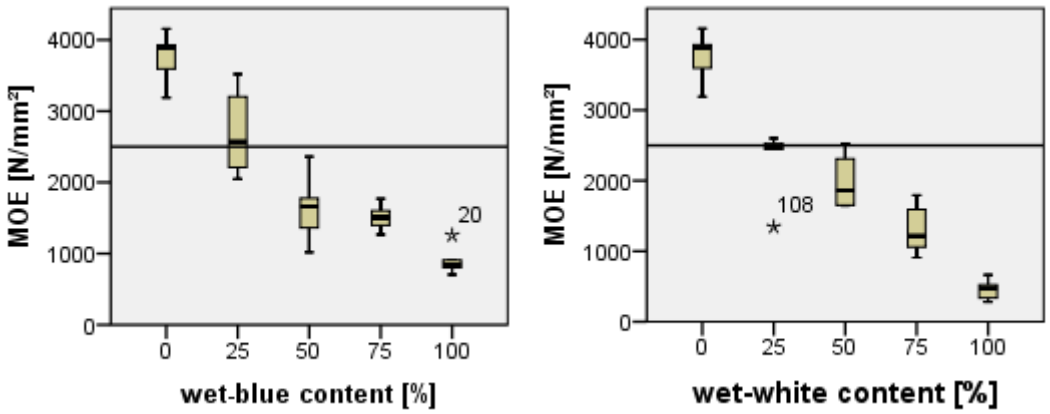

Fig. 4. Modulus of elasticity of wet-blue (left) and wet-white (right) fiberboard

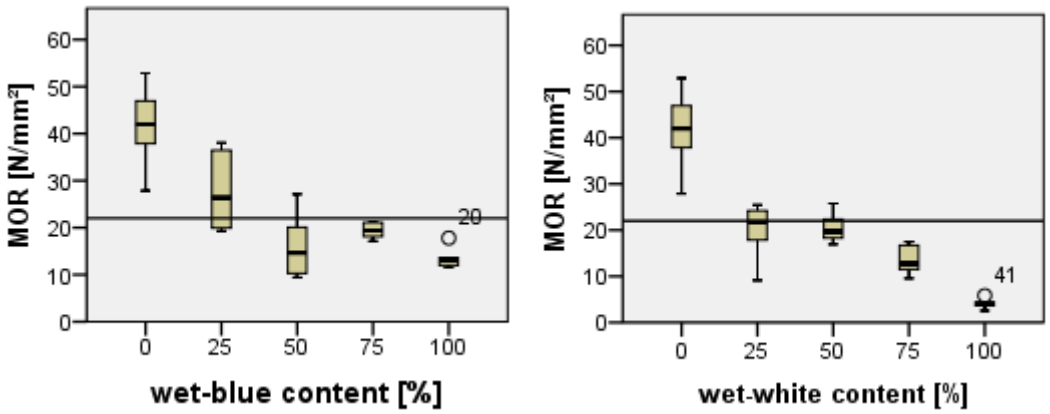

Fig. 5. Modulus of rupture of wet-blue (left) and wet-white (right) fiberboard

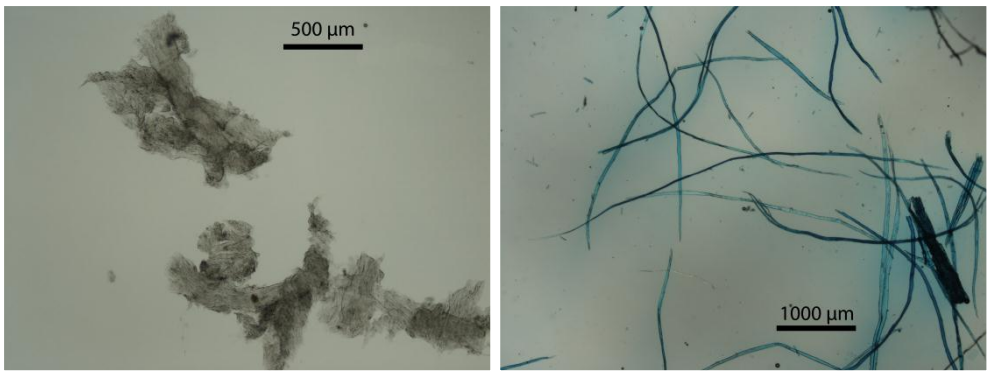

Fig. 6. Comparison between wet-blue particles (left) and wood fibers (right)

Figure 6 shows microscopic images of the used wet-blue particles and wood fibers. Figures 7 and 8 depict the fracture zones obtained by the IB tests for WB and WW panels. The leather content is rising in 25% increments from the left to the right.

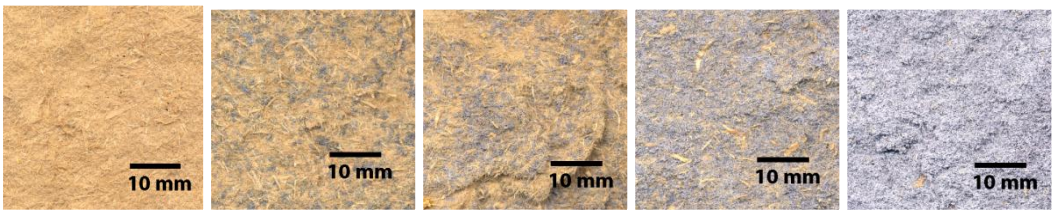

Fig. 7. Fracture zones in internal bond tests for wet-blue (left 0% WB - right 100% WB)

Fig. 8. Fracture zones in internal bond test for wet-white (left 0 % WW - right 100% WW)

Figure 9 depicts the fracture zone obtained by three-point bending tests for WB and WW. The leather content is rising in 25% increments from the top to the bottom.

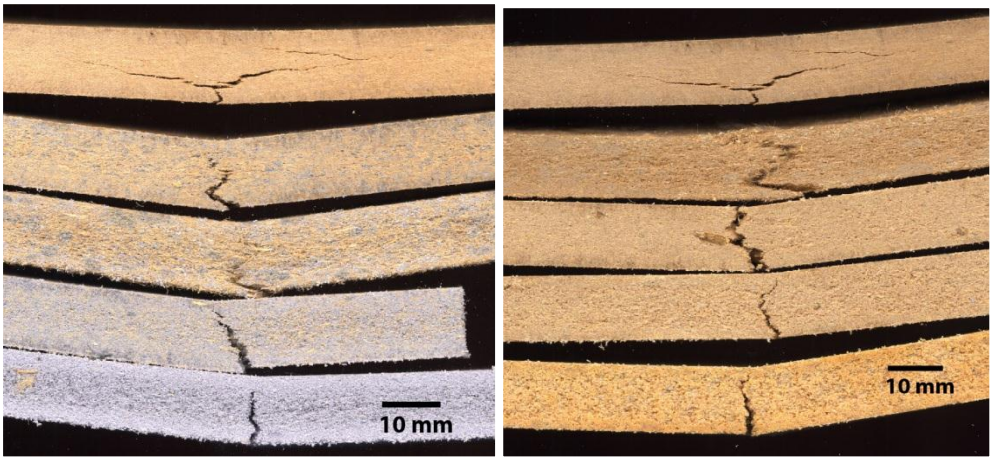

Fig. 9. Fracture zones of bending tests for wet-blue (left) and wet-white (right) fiberboards

Pore Size Distribution

Figure 10 shows the histogram of the 25% WB image stack. The arrows indicate the respective thresholds.

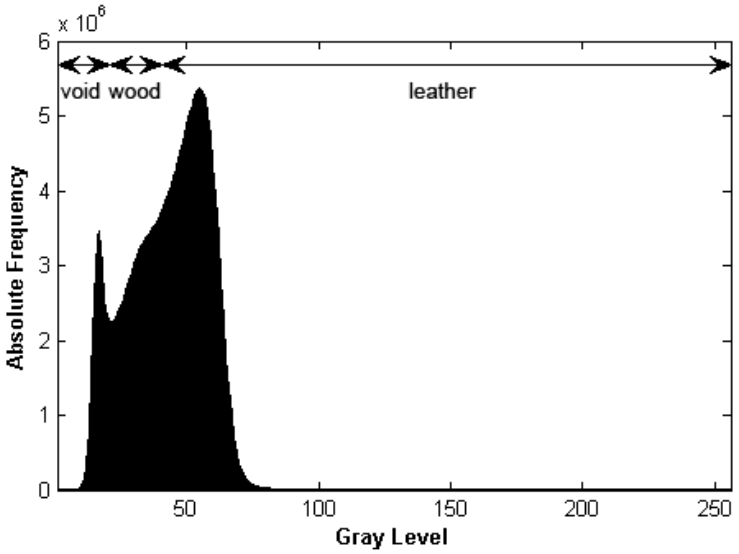

Fig. 10. Gray level histogram of the whole 25% WB image stack

Figure 11 shows a CT image of a 25 % WB panel (A) and the segmentation of its respective constituents: void (B), leather (C), and wood (D). The contrast of the CT image (a) has been enhanced for this paper to increase the visibilty.

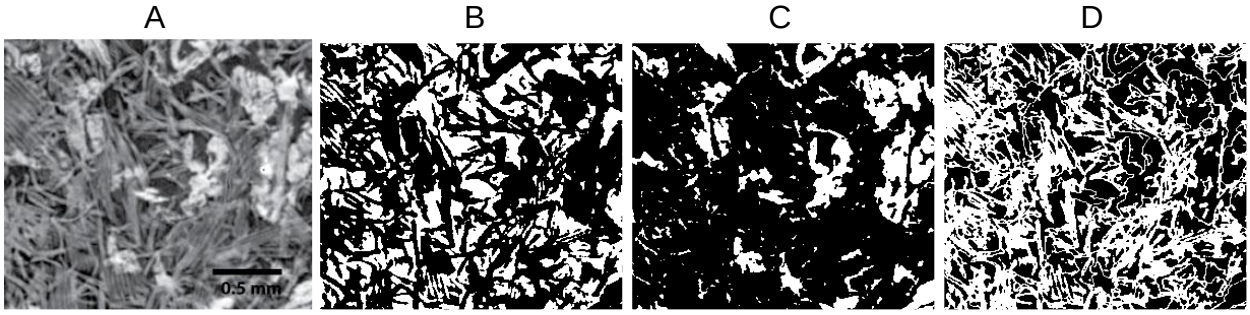

Fig. 11. CT Image (enhanced contrast for visibility) and the segmented parts of void (B), leather (C), and wood (D), each showing an area of 2.235 x 1.972 mm

Given in Table 9 are the structural properties of the 25% and 75% WB fiber boards as determined by the analysis of the CT images.

Table 9. Structural Properties of 25% and 75% WB Fiberboard

	Total Count of Pores	Average Pore Size [µm] (sd)
25% wet-blue face	4,009,381	51 (20)
25% wet-blue core	6,030,348	60 (31)
75% wet-blue face	2,769,750	57 (28)
75% wet-blue core	2,272,276	79 (42)

Figure 12 depicts the pore size distribution in the face layer of 25% and 75% WB fiberboards, whereas Fig. 13 shows the distribution in the core layer of the respective fiberboards.

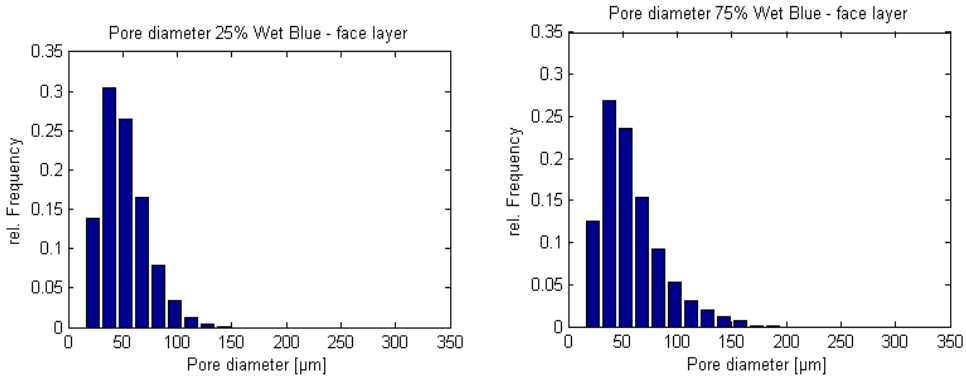

Fig. 12. Pore size distribution in the face layer of 25% and 75% wet-blue fiberboard

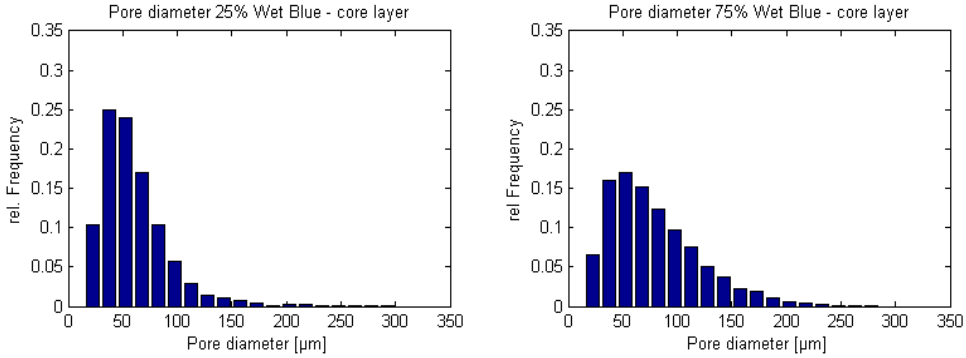

Fig. 13. Pore size distribution in the core layer of 25% and 75% wet-blue fiberboard

DISCUSSION

Mechanical Properties

The IB tests, as shown in Fig. 3 and Table 1, show an interesting relation between leather content and the IB, resulting in an increased IB for high leather contents compared to the 100% wood fiber panels. The lowest IB values were obtained for 25% WW and 50% WB, respectively. Given in Fig. 4 and 5 are the results for the MOE and MOR tests. The lines in the graphs indicate the requirements given by the standards. In the case of MOE and MOR a rather linear decline can be seen for rising leather contents. In the present case, the standards requirements could only be met at low leather contents of 25%.

Tables 2 to 7 give the statistical tests for significant differences by a Welch-ANOVA. It can be seen that although not all consecutive groups show significant differences, the influence of leather can be seen at higher contrasts levels (0% leather: 50% leather: 100% leather). Demonstrated by the analysis of covariance is the overriding influence of the leather percentage on the mechanical values, although the influence of density should not be denied, as it accounts also for some of the explanatory content.

Figure 6 gives a comparison of the geometric properties of the WB particles (WW are quite similar in geometry) and the wood fibers used for the panel preparation. The differences in the morphology are readily visible. The WB particles appear to be nearly cubic in structure, whereas the wood fibers are really fiber-like. This gives the ground for an explanation of the mechanical properties based on the geometry of the constituents.

By assessing the IB fracture zones in Fig. 7 and 8, one can see a smooth fracture for no or low leather contents. For higher leather contents one can see an increasingly

rough fracture zone. Within the transition from smooth to rough, 25% WW and 50% WB show signs of delamination in the fracture zones.

The literature (Krug 2010) states that the fracture within conventional MDF appears in zones of the lowest density in a rather smooth manner. This behavior can also be observed in the present case and can be explained by the anisotropic behavior of the fibers, as the long fibers lead to a "non-woven" fabric and layer-like structure. The fracture is therefore mostly determined by the density rather than other interaction effects. As the leather particles differ substantially with regard to their geometry, differences in the mode of fracture have to be taken into consideration, as described by Rösler *et al.* (2006). In this case, the weakest zones are mostly dominated by glue/particle interaction, as the particles show no anisotropy.

This behavior can also be observed in the fracture zones of the MOR specimens in Fig. 9. A clear transition between the ductile, fiber-dominated fracture mode of the wood fiber boards and the brittle fracture mode of the WB and WW boards (Steger *et al.* 1988) can be observed.

Another influencing factor of the mechanical properties could be related to the chemistry of the leather, which may impact the curing reaction of the resin. It is known that the curing of UF resin is induced and controlled by the acidity of the glue (Dunky and Niemz 2002). The common formulations are adapted to the environment and buffering capacity of a woody substrate, which is usually mildly acid (*e.g. Picea abies* has a pH of 4.9 (Fengel and Wegener 2003)). Leather, in general, also shows an acidic environment but differs with regard to the used tanning agent. To clarify these possible influences, further studies will be carried out.

Pore Size Distribution

Figure 10 shows a gray scale histogram of the whole 25% WB CT image stack. In this study, the main goal was to investigate the pores within the panels and seek differences within the structure of the pore size distribution.

The histogram shows a trimodal distribution. It has to be acknowledged that only the first peak, representing the void, is clearly different, whereas the other two peaks are not readily distinguishable. Therefore, only the distribution of the void was further analyzed. A differentiation of the two constituents wood and leather would need a more sophisticated local thresholding algorithm, as they do not differ enough with regard to their absorption. The respective boundaries for the three phases of void, wood, and leather are shown in Fig. 10, but only the segmented void was used for further analysis. Consequently the distribution of the other two constituents could not be assessed further.

Based on the segmented pictures, the pore size distribution could be calculated for a growing structuring element, as depicted in Fig. 2. With respect to geometric differences of wood fibers and leather particles visualized in Fig 6, it was assumed that a volume made of large, but cubic particles account for fewer but larger voids, whereas a volume made of small but long fibers show many smaller voids. As wood-based panels always have density differences between the face and the core layer, this differences and its impact has to be taken into consideration. Therefore, a sample from the dense face layer as well as a sample from the lesser dense core layer were analysed.

Shown in Table 8 and Fig. 12 and 13 are pore size distribution, their averages, and the overall count. It can be seen that 25% and 75% WB only differ little with regard to the pore diameter, but 25% WB showed a higher pore count. A possible reason for the similarity in the pore size distribution could be the usual strong compression of the face layer, leading in both cases to an homgeneous distribution. The differences in the count of pores can be attributed to the differences between leather and wood with regard to their void space, as descibed above.

The core layer showed a clear distinction in count and distribution of the pores. It was apparent that there were more smaller pores in the 25% WB material than in the 75% WB material, which shows fewer pores in a more even distribution. Although the average pore sized differed much more compared to the face layer. However, in all cases the high standard deviation has to be taken into account. Therefore, it is hard to deduce final statements from this investigation.

CONCLUSIONS

On basis of the results described above and the information gathered from literature, the results can be summarized as follows:

1. The results of the internal bond (IB) tests showed an interesting relation between leather particle and wood fiber content resulting in a 30 to 40% increase in IB for high leather contents compared to the 100% wood fiber panels. However, the IB strength showed a non-linear behavior. Therefore, further investigations *e.g.* on the particle and fiber orientation are needed to obtain a more refined understanding of these findings and the particle/fiber interaction.
2. Contrary to the IB results, the results for modulus of elasticity (MOE) and of rupture (MOR) decreased linearly with increasing leather content. For MOE and MOR the standard requirements could only be met at low leather contents of 25%. This is attributed to differences in the behavior of particle- and fiber-dominated materials. To explain and understand this behavior better, more parameters need to be tested.
3. Regarding the results of the pore size distribution, differences between the core and the face layer of the panels could be seen. The core layer showed a clear distinction in count and distribution of the pores. There were more smaller pores in the 25% WB material than in the 75% WB material, which showed fewer pores in a more even distribution. However, the average pore size differed much more compared to the face layer.
4. The presented research work proved the feasibility to produce medium density panels out of WW and WB leather particles in combination with wood fibers. With regard to the mechanical properties, the best combinations could be seen for both mixtures (25% WB/75% wood fiber and 50% WW/50 % wood fiber). To pass the standard in all three cases (IB, MOR, and MOE) a further optimization of the gluing and pressing parameters as well as a better understanding of the particle/fiber interaction is necessary.
5. The presented findings, the availability, and known properties of the leather particles as well as the determined panel properties like fire retardance (Wieland 2012) and water sorption behavior (Ostrowski 2012) show a good potential for material application in wood-based panels *e.g.* in wood fiber ceiling panels. Thus, future research should be dedicated to these fields of application.
6. With regard to the increasing scarcity of wood as a raw material, the present study showed a promising new raw material source.

ACKNOWLEDGMENTS

The authors are grateful for the support of the Austrian Research Promotion Agency (FFG) under grant no. 613108. CT scans were funded by the K-Project for non-destructive testing ZPT, grant no. 820492.

REFERENCES CITED

Ambrósio, J. D., Lucas, A. A., Otaguro, H., and Costa, L. C. (2011). "Preparation and characterization of poly (vinyl butyral)-leather fiber composites," *Polym. Compos.* 32(5), 776-785.

Backhaus, K., Erichson, B., Plinke, W., and Weiber, R. (2005). "Multivariate analysemethoden," 11th Ed., Springer-Verlag, Berlin, Heidelberg, New York.

Botting, M. (2011). "Focus on MDF," *Wood based Panels International* 31(3), 14-17.

CEN (2005), OEnorm EN 310. "Particleboards and fiberboards – Determination of tensile strength perpendicular to the plane of the board"

CEN (2005), OEnorm EN 319. "Wood-based panels – Determination of modulus of elasticity in bending and bending strength"

Dunky, M., and Niemz, P. (2002). *Holzwerkstoffe und Leime. Technologien und Einflussfaktoren*, 1st Ed., Springer-Verlag, Berlin, Heidelberg.

European Panel Federation. (2008). Annual Report 2008/2009.

Fengel, D., and Wegener, G. (2003). *Wood: Chemistry, Ultrastructure, Reactions*, Verlag Kessel, Remagen-Oberwinter.

Grünewald, T., Ostrowski, S., Petutschnigg, A., Musso, M., and Wieland, S. (2012). "Structural analysis of wood-leather panels by Raman spectroscopy," *BioResources* 7(2), 1431-1439.

Han, G., Umemura, K., Zhang, M., and Honda, T. (2001). "Development of high-performance UF bonded reed and wheat straw medium density fiberboard," *J. Wood Sci.* 47(5), 350-355.

Kanagaraj, J., Velappan, K. C., Chandra Babu, N. K., and Sadulla, S. (2006). "Solid wastes generation in the leather industry and its utilization for cleaner environment - A review," *J. Sci. Ind. Res.* 65, 541-548.

Krug, D. (2010). "Einfluss der Faserstoff-Aufschlussbedinungen und des Bindemittels auf die Eigenschaften von mitteldichten Faserplatten (MDF) für eine Verwendung im Feuch- und Außenbereich," *Disseration, Universität Hamburg*, Hamburg.

Lackinger, G. (2009). "Composite body," Patent applied for by Vogl, W., on 17/06/2009. App. no. EP 09007907.0. Patent no. EP 2135892 A2.

Lee, S., Shupe, T. F., and Hse, C. Y. (2006)."Mechanical and physical properties of agro-based fiberboards," *Holz Roh Werkst.* 64(1), 74-79.

Leiva, P., Ciannamea, E., Ruseckaite, R. A., and Stefani, P. M. (2007). "Medium-density particleboards from rice husks and soybean protein concentrate," *J. Appl. Polym. Sci*106(2), 1301-1306.

LMC International (2007). "Global Supply of hides and skins," In: *Pocket Book for the Leather Technologist*, BASF, p. 47.

Mang, H. A., Eberhardsteiner, J., Hellmich, C., Hofstetter, K., Jäger, A., Lackner, R., Meinhard, K., Müllner, H.W., Pichler, B., Pichler, C., Reihsner, R., Stürzenbecher, R., and Zeiml, M. (2009)."Computational mechanics of materials and structures," *Engineering Structures* 31(6), 1288-1297.

Mantau, U., *et al.* (2010). "Wood resource balance results - Is there enough wood for Europe?" In: U. Mantau *et al.* (eds.): *Real potentials for Changes in Growth and Use of EU Forests*, University of Hamburg, pp. 19-34.

Matheron, G. (1975). *Random Sets of and Integral Geometry*, Wiley, New York.
Ostrowski, S. (2012). "Development of an insulation material composed of natural materials .wood and leather," *Master Thesis, Salzburg University of Applied Sciences*, Salzburg.
Otsu, N. (1979)."A threshold selection method from gray-level histograms," *IEEE Trans. Systems, Man and Cybernetics* 9, 62-66.
Ramaraj, B. (2006)."Mechanical and thermal properties of ABS and leather waste composites," *J. Appl. Polym.Sci* 101(5), 3062-3066.
Rösler, J., Harders, H., and Bäker, M. (2006). *Mechanisches Verhalten der Werkstoffe*, 2nd Ed., B. G. Teubner, Wiesbaden.
Serra, J. (1982). *Image Analysis and Mathematical Morphology*, Academic Press, London.
Standfest, G., Kranzer, S., Petutschnigg, A., and Dunky, M. (2010)."Determination of the microstructure of an adhesive-bonded medium density fiberboard (MDF) using 3-D sub-micrometer computed tomography," *J. Adhes. Sci. Technol.* 24, 1501-1514.
Standfest, G., Petutschnigg, A., and Dunky, M. (2009)."2D pore size distribution in particleboard and oriented strand board," In: Proc. ISPA09 (Proceedings of the 6th International Symposium on Image and Signal Processing) 6, pp. 359-364.
Steger, H., Sieghart, J., and Glauninger, E. (1988). *Technische Mechanik 2*, B.G. Teubner, Stuttgart.
Sundar, V. J., Gnanamani, A., Muralidharan, C., Chandrababu, N. K., and Mandal, A. B. (2011). "Recovery and utilization of proteinous wastes of leather making: A review," *Rev. Environ. Sci .Biotechnol.*10(2), 151-163.
Wieland, S., Stöckl, U., Grünewald, T., and Ostrowski, S. (2012). "Wood-leather panels – A biological, fire retardant building material," In: Proc. 2012 IUFRO Conference, Division 5, pp. 139-140.

Article submitted: July 27, 2012; Peer review completed: September 29, 2012; Revised version received and accepted: December 18, 2012; Published: December 19, 2012.